Types of temperature dependence of single-ion magnetic anisotropy constants by general thermodynamic considerations

Yonko Millev* and Manfred Fähnle
Institut für Physik, Max-Planck-Institut für Metallforschung, Heisenbergstrasse 1, 70569 Stuttgart, Federal Republic Germany
(Received 16 February 1995)

A general discussion of the temperature dependence of the magnetic anisotropy of single-ion origin is given based on the connection between the experimentally measured anisotropy constants and the theoretically more fundamental anisotropy coefficients. The cases of uniaxial and cubic crystal symmetry are considered in turn and the qualitative and quantitative differences between them are treated. General analytical arguments valid for at least a whole class of untrivial collective-excitation theories including the mean-field theory are implemented to describe exhaustively the types of temperature dependence of the anisotropy constants in the two-parameter phenomenological expression for the free energy. Anisotropy-flow diagrams in the plane $(K_1 - K_2)$ are given for both the uniaxial and the cubic cases. In both cases, three crossover-inducing wedges have been detected in the anisotropy phase diagram. A system which resides in one of these wedges at $T = 0$ inevitably runs away to a phase with another easy-axis orientation at some spin-reorientation temperature T_S when the temperature is increased. T_S is determined for some representative cases. In the experimentally interesting case when a uniaxial system evolves from a tilted axis to an easy axis along the c axis or in an easy plane perpendicular to it, the temperature dependence of the cone angle $\theta(T)$ is given and a critical angle θ_{cr} resolving between the two possible crossover scenarios is determined. Prospective generalizations and applications are described for the implementation of the general procedures to the characterization of anisotropy in technologically important hard magnetic materials as typified by $Nd_2Fe_{14}B$.

I. INTRODUCTION

It is the purpose of this paper to show that very general theoretical arguments lead to the prediction of a variety of possibilities for the temperature dependence of the experimentally measured magnetic *anisotropy constants* which rank among the most extensively studied and important properties of magnetic materials. On one hand, this variety is in itself a much desired qualitative match to the corresponding variety of experimental temperature behavior of anisotropy. On the other hand, the proposed method has the power to introduce quite generally quantitative systematics into this variety. The analysis is carried out by using the connection between the respective sets of anisotropy *constants* and anisotropy *coefficients*. The set of constants arises when one implements the phenomenological thermodynamic expansion of the direction-dependent part of the free energy in powers of direction cosines, while the set of coefficients corresponds to the expansion of the same quantity in spherical harmonics. The constants are the ones measured in experiment, while the coefficients are theoretically much more convenient because of their superior transformation properties.[1–3] The set of coefficients is also the more fundamental one, because it emerges naturally at the statistical mechanical level of treatment of magnetic anisotropy, where one starts with the formulation of the relevant quantum mechanical Hamiltonian and proceeds with the development of the thermodynamics by eventually computing the partition function. The fundamentality of the anisotropy coefficients is then seen to stem from the group-theoretical classification of the spin operators describing the magnetic anisotropy at the quantum mechanical level. An enlightening description of the possible levels of treatment of magnetic anisotropy and magnetostriction can be found in Ref. 4.

Prototype substances to which the following discussion of single-ion anisotropy applies immediately are all those cases where there is a well-defined single-ion contribution to the overall anisotropy coming from magnetic rare-earth (RE) ions. However, the described procedures are certainly applicable to other cases of anisotropic materials where anisotropy-producing mechanisms may still be cast in the form given in the next section, although for them there might not exist a rigorous justifying procedure comparable to the well-established operator-equivalent method.[5,6]

II. STATISTICAL TREATMENT OF ONE-ION ANISOTROPY

As is well known, the partition function can be calculated exactly only in rare cases or under special unrealistic assumptions. To the purposes of treatment of magnetic anisotropy, however, there are quite general and

commonly met conditions under which a first-order thermodynamic perturbation theory produces rather satisfactory quantitative results. This is the dominant-exchange-interactions case when the crystal-field anisotropy terms are much smaller than the quantum-mechanical exchange, usually represented as a Heisenberg-exchange term in the Hamiltonian, which is responsible for the strong magnetic behavior of the system of interacting moments.[1,3] The starting point is then the Hamiltonian

$$\hat{\mathcal{H}} = \hat{\mathcal{H}}_0 + \hat{\mathcal{H}}_A \ , \tag{1}$$

where the bare part contains the dominant exchange interaction and, in an applied magnetic field, the Zeeman term, while $\hat{\mathcal{H}}_A$ is the anisotropy part and may, in principle, contain one-ion and two-ion contributions. The latter will not be our concern. In the first-order perturbation theory they contribute additively to the anisotropy constants, whereby sufficiently general and satisfactory information about the temperature dependence of the two-ion contribution has now long been known and applied successfully.[7–9]

Treating the one-ion anisotropy within the spin-operator-equivalents method,[5,6] one finds for $\hat{\mathcal{H}}_A$ the expansion in Stevens' operators $\hat{O}_n^m$:

$$\hat{\mathcal{H}}_A = \sum_n \sum_{m=-n}^{+n} B_n^m \hat{O}_n^m \ . \tag{2}$$

The free energy corresponding to the Hamiltonian from Eqs. (1) and (2) in the first-order perturbation theory is then simply

$$F = F_0 + F_A \tag{3}$$

with the anisotropy energy

$$F_A = \sum_n B_n^o \langle \hat{O}_n^o \rangle Y_n^o(\theta), \tag{4}$$

where $\langle \cdots \rangle$ denotes averaging with respect to the bare (dominant-exchange plus Zeeman) part in Eq. (1), Y_n^o is the corresponding spherical harmonic, and θ is the angle between the magnetization and the z-axis which is usually taken along one of the principal crystallographic directions. In deriving Eq. (4), cylindrical symmetry has been assumed.[1,3] This means that one neglects anisotropy effects in the plane perpendicular to the z axis. This restriction is not dramatic, because only a few $B_n^m (m \neq 0)$ are nonzero and because the in-plane anisotropy is usually negligible or is averaged out due to special experimental circumstances.[10] Considering only $m = 0$ would help emphasize the most general features of the analysis which lead to different *types of temperature dependence of the anisotropy constants* and which would otherwise be blurred by an unnecessary complication.

There are important restrictions which are implicit in the expression (4) and which have different physical sources. One such group of restrictions originates in the general quantum-mechanical properties of angular momentum operators. The summation in n is over even integers because of the time-reversal symmetry; conventionally, it starts from $n = 2$, since the term with $n = 0$ provides for a constant rather than for an angle-dependent contribution to F_A. On the other hand, for any given angular momentum number the highest independent power of any angular operator is $2J + 1$ because of the well-known commutation relations. Combining both requirements means that the sum in Eq. (4) runs from 2 to $2p$ with

$$p = [J] \ , \tag{5}$$

$[J]$ being the integer part of J.

A further important and very significant restriction exists for the above-mentioned prototype case of RE-ion dominated anisotropy. It can be traced back to the properties of the $4f$-electron charge density. In fact, the f electrons with an individual orbital momentum of 3 cannot have multipole distributions of order greater than 6 (in calculating the average of the crystal-field perturbation over the electronic states, all matrix elements with $m_j > 3$ will be zero for f electrons).[11] In other words, all $B_n^m (n > 6)$ are then identically zero. Finally, crystal symmetry also imposes strict conditions. Not only does it determine the type of $B_n^m (m \neq 0)$ for a given n, but it requires that in cubic symmetry B_2^m (any m) be identically zero.

With these assumptions, the anisotropy free energy is

$$F_A = \sum_{n=2}^{2p} B_n^o \langle \hat{O}_n^o \rangle Y_n^o(\theta) \tag{6}$$

with $p = [J]$ as explained above. It is assumed that we have only one magnetic sublattice to worry about. The way to relax this restriction in some technologically important hard magnets will be discussed later. Besides, in many important cases the contributions from different sublattices can be accounted for additively.[12,13]

Now we introduce the magnetic *anisotropy coefficients*[1,14]

$$\bar{\kappa}_n(T) \equiv \frac{\langle \hat{O}_n^o \rangle (T)}{\langle \hat{O}_n^o \rangle (0)} \tag{7}$$

as the thermal averages of the Stevens' operators normalized against their zero-temperature values. The bar is to remind of this normalization. The zero-temperature values are certain J-dependent products which will henceforth be denoted as $p_n(J)$. Both $\bar{\kappa}_n$ and $p_n(J)$ can be computed from Table IX of Ref. 6 with the result

$$\begin{aligned}
\bar{\kappa}_2 &= \frac{1}{p_2(J)}[3M_2 - J(J+1)], \\
\bar{\kappa}_4 &= \frac{1}{p_4(J)}[35M_4 + (25 - 30J - 30J^2)M_2 \\
&\quad + 3J^2(J+1)^2 - 6J(J+1)] \ , \\
\bar{\kappa}_6 &= \frac{1}{p_6(J)}\{231M_6 + [735 - 315J(J+1)]M_4 \\
&\quad + [294 - 525J(J+1) + 105J^2(J+1)^2]M_2 \\
&\quad - 60J(J+1) + 40J^2(J+1)^2 - 5J^3(J+1)^3\} \ ,
\end{aligned} \tag{8}$$

where

$$M_n \equiv \langle (\hat{J}_z)^n \rangle \tag{9}$$

are the moments of the operator $\hat{J}_z$ computed with the bare Hamiltonian $\hat{\mathcal{H}}_0$. The products $p_n(J) \equiv \langle \mathcal{O}_n^o \rangle (T = 0)$ are:

$$\begin{aligned} p_2(J) &= 2J(J-\tfrac{1}{2}), \quad J > \tfrac{1}{2}; \\ p_4(J) &= 8J(J-\tfrac{1}{2})(J-1)(J-\tfrac{3}{2}), \quad J > \tfrac{3}{2}; \\ p_6(J) &= 16J(J-\tfrac{1}{2})(J-1)(J-\tfrac{3}{2}) \\ &\quad \times (J-2)(J-\tfrac{5}{2}), \quad J > \tfrac{5}{2} \, . \end{aligned} \tag{10}$$

The bound for J from below in the last equations derives from the general properties of the Stevens' operators. The important point is that all moments M_n and, consequently, all $\bar{\kappa}_n$'s can be expressed via the first moment M_1 (or, equivalently, via the reduced magnetization per site $m = M_1/J$)

$$M_1(x) = JB_J(Jx) \tag{11}$$

for a whole class of untrivial collective-excitation theories.[15] This theorem will be substantial below. In the last equation, $B_J(y)$ is the Brillouin function, while x is the generalized effective field related to the average number $\Phi(T)$ of magnetic quasiparticle excitations.[15]

One thus comes to the very important representation of the anisotropy part of the free energy of one-ion origin as a linear combination of a restricted number, not greater than p, of the functions $\{\bar{\kappa}_n\}$ which carry the temperature dependence of F_A:

$$F_A = \sum_{n=2}^{2p} B_n^o p_n(J) Y_n^o(\theta) \bar{\kappa}_n(T) \, . \tag{12}$$

Note that it is exactly the role of $\{\bar{\kappa}_n\}$ as a finite, normalized basis which spans the temperature dependence of anisotropy which is important here and below.

III. TWO REPRESENTATIONS FOR THE MAGNETIC ANISOTROPY ENERGY: ANISOTROPY CONSTANTS AND ANISOTROPY COEFFICIENTS

The form (12) is the output of the perturbative statistical treatment of the microscopic problem of interacting magnetic moments. It has to be compared with the phenomenological expression for the anisotropy energy as a symmetry-dictated expansion in direction cosines of magnetization with respect to the crystal axes. These expansions have been known for quite some time.[16]

A. Uniaxial case

Let us first discuss in greater detail the uniaxial case. Neglecting once again the in-plane anisotropy, the phenomenological expression reads

$$F_A' = K_1 \sin^2\theta + K_2 \sin^4\theta + K_3 \sin^6\theta + \cdots \, . \tag{13}$$

The temperature behavior is now carried by the anisotropy constants $\{K_i(T)\}$ and the tacit assumption is that there are infinitely many of them. There immediately arises the problem of how many terms one must keep in this expansion. Order can be brought into the discussion by simply noting that $F_A = F_A'$, so far as only the purely angular part is envisaged in both cases. Simple argument based on the orthogonality properties of $Y_n^o(\theta)$ and $\sin^{2l}\theta$ shows that the highest admissible power of $\sin\theta$ in the phenomenological expression is exactly $2p$. This means that the one-ion phenomenological anisotropy expansion Eq. (13) has only a few terms (their number is at most $p = [J]$ and this can only be infinity in the classical case of $J = \infty$). Therefore, one must clearly recognize the fact that F_A' from Eq. (13) is *a finite-term trigonometric expression.* Hence

$$F_A' = K_1 \sin^2\theta + K_2 \sin^4\theta + \cdots + K_p \sin^{2p}\theta \tag{14}$$

with the same p ($p = [J]$) as in Eq. (6). The consideration of $B_n^m (m \neq 0)$ does not change the validity of the above italicized statement; it would only increase by a few the number of terms for any given J.

Now one is in the position to systematize the connection between the $\bar{\kappa}$'s and the K's in cylindrical symmetry for one-ion anisotropy. Starting with the highest allowed K_p, one has, generally,

$$\begin{aligned} K_p &= a_p \bar{\kappa}_{2p}, \\ K_{p-1} &= b_{p-1}\bar{\kappa}_{2(p-1)} + b_p \bar{\kappa}_{2p}, \\ &\cdots \cdots \cdots \cdots \cdots \cdots \cdots \cdots \cdots \\ K_2 &= c_1\bar{\kappa}_4 + \cdots + c_{p-1}\bar{\kappa}_{2(p-1)} + c_p\bar{\kappa}_{2p} \\ K_1 &= d_1\bar{\kappa}_2 + d_2\bar{\kappa}_4 + \cdots + d_{p-1}\bar{\kappa}_{2(p-1)} + d_p\bar{\kappa}_{2p}. \end{aligned} \tag{15}$$

These relations can also be cast in a matrix form with a triangular transformation matrix, but it is hardly necessary to do so here. The triangularity comes from the simple observation that a term of the form $K_i \sin^{2i}\theta$ in the phenomenological expansion cannot contain contributions from $\bar{\kappa}_{2j} Y_j^o(\theta)$ with j smaller than i since this would imply that K_i multiplies also terms of lower powers in $\sin\theta$ which is impossible by the definition of K_i. The coefficients in the above linear combination involving the "temperature basis" $\{\bar{\kappa}_n\}$ can all be expressed via p independent parameters.

Several words of caution are due already here. The connection between *constants* and *coefficients* is so simple only in the first-order thermodynamic perturbation theory which we are exclusively preoccupied with. Besides, in a purely phenomenological *ad hoc* approach one may use effective values of J which are not integer or half-integer at all; such an approach cannot be justified theoretically, although it may offer a better experimental fit via, say, a better correspondence between experimental and mean-field (MF) magnetization curves calculated with this arbitrary J value. Finally, if one includes

magnetoelastic effects in the Hamiltonian, terms in $\sin\theta$ which are of order higher than $2p$ may arise in the phenomenological expansion.[3,17] The same would happen if one proceeds with higher orders of the perturbation theory.

Leaving aside for the time being magnetoelastic effects and unjustifiable values of J, it is important to note that the application of the system of linear combinations (15) is subject, via the connection with the coefficients $\bar{\kappa}_n$, to the same restrictions as the application of F_A from Eq. (12). At this point, some thought leads to the simple but important corollary that a given p-constant expression for F'_A is strictly relevant for only two values of J: $J = p$ and $J = p + \frac{1}{2}$. One may want to know the answer to the inverse question: given a half-integer or integer J, how many terms must be included in the phenomenological expression for F'_A? Summarizing the above considerations, the answer is that one needs either $p = [J]$ terms if J is a fictitious quantum number whose most prominent characteristic is that the number $2J + 1$ accounts for the correct multiplicity of the relevant lowest-lying spectroscopic levels,[18] or else $p' = \min(3, [J])$ for any J if one is dealing with single-ion anisotropy originating from the *nominal* quantum angular momenta of RE ions.

The representation (15) is paramount to the understanding of the general underlying reasons determining the temperature dependence of the anisotropy *constants*. First, as already emphasized, there is only a limited number p of anisotropy constants for a given J. Second, the greater the index i ($i = 1, 2, \ldots, p$), the smaller the number of the basic ingredients $\{\bar{\kappa}_j\}$. The immediate corollary is that the most rich temperature behavior as regards possible types of temperature dependence of the anisotropy constants is to be expected and observed, in principle, for the first constant K_1 in the phenomenological expansion for F'_A. The fact that this is really the case has been recorded many a time, but it appears that no one has tried to explain simply and generally this state of matters. Third, the parameters $\{a; b; \ldots; c; d\}$ in Eqs. (15) have the dimension of energy per volume and set both the *scale* and the *sign* of the contribution of the respective normalized and positive temperature dependent ingredients $\bar{\kappa}_{2l}(T)$ ($0 \leq \bar{\kappa}_{2l} \leq 1$ for $T_c \geq T \geq 0$), thus allowing for the possible variety just mentioned. Besides, all these parameters can be expressed via p basic parameters only. The basic set can be chosen as the set of p parameters B_n^o ($n = 2, 4, \ldots, p$).[3] An even more straightforward and experimentally appealing choice will be discussed below.

Furthermore, if some of the allowed terms in F'_A have been thrown overboard in a certain anisotropy analysis, the relations (15) provide insight and control on what exactly has been neglected by doing so. Finally, the highest possible constant K_p is simply proportional to $\bar{\kappa}_{2p}$ which should facilitate the estimation of its contribution at different temperatures.

B. Cubic case

For the case of *cubic* symmetry, the phenomenological expansion $F_A^{c\prime}$ is

$$F_A^{c\prime} = K_1(\alpha_1^2\alpha_2^2 + \alpha_2^2\alpha_3^2 + \alpha_3^2\alpha_1^2) + K_2(\alpha_1\alpha_2\alpha_3)^2 + \cdots , \tag{16}$$

where the α's are the direction cosines of the magnetization with respect to the reference frame whose z axis is usually along a principal crystallographic direction.[14,16] The $\bar{\kappa}$ representation of the K_i's proceeds quite analogously to Eq. (15). The natural enumeration of the anisotropy constants starting from the highest K_i meets the trifling complication that here B_2^o and, hence, the contribution from $\bar{\kappa}_2$ are identically zero, so that the first constant K_1 starts with a term proportional to $\bar{\kappa}_4$. To keep up in accord with the existing literature, it is natural to shift by one some of the indices as given below:

$$\begin{aligned}
&K_{p-1} = a_{p-1}\bar{\kappa}_{2p}, \\
&K_{p-2} = b_{p-2}\bar{\kappa}_{2(p-1)} + b_{p-1}\bar{\kappa}_{2p}, \\
&\cdots\ \cdots\ \cdots\ \cdots\ \cdots\ \cdots\ \cdots\ \cdots\ \cdots \\
&K_2 = c_2\bar{\kappa}_6\ + \cdots + c_{p-2}\bar{\kappa}_{2(p-1)} + c_{p-1}\bar{\kappa}_{2p}, \\
&K_1 = d_1\bar{\kappa}_4\ + d_2\bar{\kappa}_6 + \cdots + d_{p-2}\bar{\kappa}_{2(-1)} + d_{p-1}\bar{\kappa}_{2p}.
\end{aligned} \tag{17}$$

It is to be understood that the parameters $\{a; b; \ldots; c; d\}$ are different from those in the corresponding system of relations for the uniaxial case (15). One observes that, quite generally, the allowed number of constants in the cubic case is one less than the corresponding number in the uniaxial case for a given value of J and that the linear combination of $\bar{\kappa}_l$'s for a given K_j is one term shorter in cubic symmetry than in uniaxial symmetry for the same value of J. This implies relatively restricted possibilities for the temperature variation in the cubic case as compared with the uniaxial one. Now all parameters $\{a; \ldots; d\}$ can be expressed, in principle, via the set of $p - 1$ parameters B_n^o ($n = 4, \ldots, 2p$) or via an equivalent suitable set to be introduced shortly. Once again, if one considers $4f$-electron anisotropy and not a fictitious J, the situation is much simpler. The one-constant anisotropy energy is exhaustive for $J = 2$ and $5/2$, while the two-constant expression for the free energy is adequate for any $J \geq 3$. The reason is that only B_4^0 and B_6^0 would be nonzero, and correspondingly only $\bar{\kappa}_4$ and $\bar{\kappa}_6$ would contribute, if the one-ion anisotropy comes from a rare-earth ion sitting on a site of cubic symmetry. In other words, the one-ion anisotropy of rare-earth ions in a locally cubic environment is adequately described by a two-constant $F_A^{c\prime}$. This observation makes the following analysis of the two-parameter cubic case rather conclusive under the described circumstances. In this way, already the qualitative analysis brings forward important differences between the uniaxial and cubic cases. Further insights will be gained by carrying out the quantitative investigation in each of the symmetries (see Sec. V).

IV. THE IMPORTANCE OF THE ZERO-TEMPERATURE VALUES K_i^o OF THE ANISOTROPY CONSTANTS $K_{i(T)}$

At this place we introduce the following simple idea which allows an immediate connection of the general analysis as given above with experimental measurements of one-ion anisotropy on specific substances. We namely

choose as independent parameters the set of quantities

$$K_i^o \equiv K_i(T=0) \tag{18}$$

($1 \le i \le p$ in the uniaxial case; $1 \le i \le p-1$ in the cubic case). In other words, the chosen parameters are the *intrinsic* anisotropy constants. On one hand, the K_i^o's fix the energy scale for the $K_i(T)$'s most straightforwardly and, at the same time, most simply. Because of the initial "flatness" of the observed and calculated temperature dependences of the $\bar{\kappa}_l$'s (all of them have a vanishing first derivative as $T \to 0$), it suffices to take the liquid-^{4}He temperature value of K_i as the zero-temperature value when magnetic materials with $T_c > 100$ K are considered and this should present no serious experimental difficulty; an extrapolation procedure would also do. Besides, the estimates of other contributions to the anisotropy of the examined substance which may come in through other anisotropy-generating mechanisms or because of another magnetic sublattice as is the case with a series of rare-earth–transition-metal–boron compounds, are especially trustworthy at $T = 0$, since general ground-state considerations are usually available and helpful. It is therefore quite appealing to develop the scheme in this experimentally-friendly way. The contact with microscopic *ab initio* calculations of the whole set $\{B_n^o\}$ is not lost, because both sets $\{K_i\}$ and $\{B_n^o\}$ are expressible through each other.[3] Therefore, one can also proceed from the *ab initio* end of the problem, whereby the energy scale for the temperature variation of the anisotropy constants K_i is set by the theoretically determined quantities B_n^o.[6] The road thus being open, in principle, for a two-way comparison and mapping, we proceed to examine the "experimental" approach from a closer distance.

V. TYPES OF TEMPERATURE VARIATION OF $K_i(T)$: GENERAL ANALYSIS

Now we shall analyze the first two possible cases (those with one and two anisotropy constants, respectively). The method can then serve as a basis for detailed analyses of more complicated particular cases and it will be seen that the difficulties in extending the method are only technical and surmountable. Besides, it will become obvious that not only is the suggested systematizing approach capable of accounting for some unusual types of temperature behavior of anisotropy, but it can also provide for an ample quantitative characterization of these types under rather general conditions.

A. Uniaxial case

1. The "trivial" uniaxial case: $p = 1$

The "trivial" case in the sense envisaged here is when only the term with K_1 is kept in the phenomenological expression (14). This case can be named the one-constant case. By Eqs. (15) with $p = 1$,

$$K_1(T) = a_1\bar{\kappa}_2 = K_1^o\bar{\kappa}_2 \ . \tag{19}$$

In view of the previous remarks, the expression $F_A = K_1 \sin^2\theta$ is exhaustive for $J = 1$ and $J = \frac{3}{2}$, since then $p = [J] = 1$ and no higher terms are allowed. Besides following the traditional argument, the same expression can be used as a reasonable approximation in materials with higher J but higher constants $K_i (i > 1)$ which are much smaller than K_1 by modulus over the temperature domain of specific interest. The expression (19) is trivial only in as much as a single temperature-dependent basis function $\bar{\kappa}_2(T)$ is used. The computation of the latter, however, is by far not trivial.[19,20] It has been found, among other things, that $\bar{\kappa}_2(T)$ is a convex-upwards function of T in the MF approximation.[19] Calculations in the random-phase approximation (RPA) to the Green's functions approach which gives the correct low-temperature behavior of magnetic anisotropy, though by now carried out for cubic symmetry only,[20] indicate that, significant as they are, the differences between the MF approximation and the much more involved RPA do not change the qualitative character of the quantities computed. That is, one should expect that the convexity of $\bar{\kappa}_2(T)$ holds beyond the MF approximation. The conclusions are thereby immediate and clear: for substances of uniaxial symmetry with $J = 1$ or $J = \frac{3}{2}$, the temperature dependence of anisotropy is given by $\bar{\kappa}_2$ as scaled by K_1^o. If K_1^o is positive, so is $K_1(T)$ over the entire range between zero and the Curie temperature T_c, while the easy direction is along the z axis. If K_1^o is negative, one finds an easy-plane anisotropy. This case exhibits the remarkable feature that it can be solved for the temperature dependence of the relevant anisotropy coefficient and constant explicitly by using the exact analytical inversion of the Brillouin function for $J = 1$ and $J = 3/2$.[21] Details of how to apply this inversion to compute $\bar{\kappa}_2(T)$ analytically and not parametrically are given in Ref. 19.

2. The two-constant uniaxial case: $p = 2$

This is the simplest untrivial uniaxial case when *two* anisotropy constants in the expression (14) are considered:

$$F_A' = K_1 \sin^2\theta + K_2 \sin^4\theta \ . \tag{20}$$

Working from top of Eqs. (15), one has

$$K_2(T) = a_2\bar{\kappa}_{2p}(T) = K_2^o\bar{\kappa}_4(T) \ ; \tag{21}$$

$$K_1(T) = b_1\bar{\kappa}_2(T) + b_2\bar{\kappa}_4(T) \ . \tag{22}$$

Here $p = [J] = 2$; hence the expression (20) is *exhaustive* for $J = 2$ and $J = \frac{5}{2}$.

Now we have to carry out the proclaimed program and express all parameters in (21) as functions of K_1^o and K_2^o. To avoid distracting discussions of the normalization of Y_n^o and B_n^o which is amply described in Ref. 22, we prefer to use as most suitable and straightforward the connection between the K's and the κ's as given for this two-constant case in Ref. 23:

$$K_1 = \kappa_2 - \frac{8}{7}\kappa_4 \ , \tag{23}$$

$$K_2 = \kappa_4 = K_2^o \bar{\kappa}_4 \ , \tag{24}$$

where the unnormalized κ's can obviously be represented as $\kappa_l = \kappa_l(0)\bar{\kappa}_l$. Examining both equations [(23) and (24)] at $T = 0$, one has two independent conditions for the two quantities $\kappa_2(0)$ and $\kappa_4(0)$. Solving for these as functions of K_1^o and K_2^o, one finds in the two-constant formalism

$$K_1(T) = \left(K_1^o + \frac{8}{7}K_2^o\right)\bar{\kappa}_2 - \frac{8}{7}K_2^o\bar{\kappa}_4 \ , \tag{25}$$

$$K_2(T) = K_2^o\bar{\kappa}_4 \ . \tag{26}$$

Thereby one easily identifies the constants b_1 and b_2 from Eqs. (21) as $b_1 = K_1^o + \frac{8}{7}K_2^o$ and $b_2 = -\frac{8}{7}K_2^o$. Using the definition of the operator equivalents $\hat{O}_n^o$ as given by Hutchings,[6] one finds for the parameters B_n^o of Eq. (2), with the normalization for Y_n^o chosen in Ref. 23,

$$B_2^o = \frac{1}{p_2(J)}\left(K_1^o + \frac{8}{7}K_2^o\right), \tag{27}$$

$$B_4^o = \frac{1}{p_4(J)}K_2^o. \tag{28}$$

The explicit connection with the microscopics is thus established. The two-parameter expressions for the one-ion anisotropy from Eqs. (25) can now be used by feeding-in either *experimental* data (K_1^o, K_2^o) or *ab initio* data (B_2^o, B_4^o). In this paper we shall consistently use the experimental onlook and take representative (K_1^o, K_2^o) values.

An important point is that if one works with the normalized constants K_1 and K_2, the temperature behavior is in fact determined by the ratio $r \equiv K_2^o/K_1^o$:

$$\frac{K_1}{K_1^o} = \left(1 + \frac{8}{7}\,r\right)\bar{\kappa}_2 - \frac{8}{7}\,r\,\bar{\kappa}_4 \ , \tag{29}$$

$$\frac{K_2}{K_2^o} = \bar{\kappa}_4 \qquad \text{or} \qquad \frac{K_2}{K_1^o} = r\cdot\bar{\kappa}_4 \ . \tag{30}$$

With this normalization, the reduced anisotropies K_i/K_i^o always start from the positive value of unity at $T = 0$. Sometimes this does not allow to grasp at once whether some of the K_i's are negative for $T \to 0$. It might therefore be advantageous to normalize against $|K_i^o|$.

It is clear that the normalization can be carried out in the general relations for the uniaxial and cubic cases (15) and (17). This will then be their most compact and expressive form, but we deliberately postponed the discussion of this point up to now in order to demonstrate the issue on the simplest example. In the general case of p allowed anisotropy constants, *the duly normalized constants depend on* $p-1$ *parameters only.* They can be chosen as

$$r_i \equiv \frac{K_i^o}{K_1^o} \qquad (i = 2, 3, \ldots, p) \ , \tag{31}$$

or

$$r_i' \equiv \frac{K_i^o}{|K_1^o|} \qquad (i = 2, 3, \ldots, p) \ . \tag{32}$$

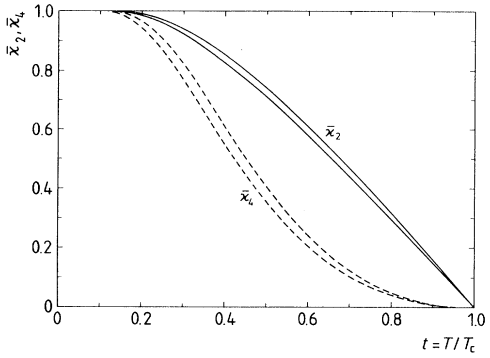

FIG. 1. Magnetic anisotropy coefficients $\bar{\kappa}_2$ and $\bar{\kappa}_4$ as functions of reduced temperature $t = T/T_c$ for $J = 2$ and $J = 5/2$ in the MF approximation. In each pair of curves the upper one corresponds to smaller J. Note the sign-invariable convexity of $\bar{\kappa}_2(T)$ over the whole range $0 \le T \le T_c$ and the existence of an inflexion point of $\bar{\kappa}_4(T)$ approximately halfway down from T_c.

That is to say, the anisotropy constants are then measured in units of K_1^o.

Now we come to the most interesting part of the application of the general method outlined in Sec. III to the two-constant (K_1 and K_2) case: the possible types of temperature behavior as given by Eqs. (29) and (30). One clearly needs the temperature dependence of the magnetic anisotropy coefficients $\bar{\kappa}_l$. For $\bar{\kappa}_2$ and $\bar{\kappa}_4$, this has been reported for the quantum case of finite J in Refs. 19 and 20. The results were found in the MF approximation for the uniaxial case and in the RPA and MF approximation for the cubic case. Any value of J can be treated within this formalism. To be consistent, at this point we prefer to give only the curves related to $J = 2$ and $J = \frac{5}{2}$ (Fig. 1) since, as explained above, the two-K analysis of one-ion anisotropy is exhaustive for these values in the first-order thermodynamic treatment. However, the temperature curves for any J for which the corresponding $\bar{\kappa}_l$ is defined can be used in an approximate approach when higher constants with $i > 2$ are allowed but have been neglected for experimental or computational reasons.

Mathematically, we are facing the problem of examining the result [K_1 from Eq.(25)] of superposing two strictly monotonically decreasing, continuously differentiable functions [$\bar{\kappa}_2(t)$ and $\bar{\kappa}_4(t)$] on the interval $0 \le t \le 1$, $t = T/T_c$. Note, however, that even in the MF approximation the temperature dependence of the $\bar{\kappa}_n$'s *is not explicit.* It has been found in a graphical and tabular form by implementing a special parametric procedure described in detail elsewhere.[19,24] Hence a self-suggesting procedure would be to study numerically or, which is the same, graphically all possible values of the ratio $r = K_2^o/K_1^o$, $-\infty \le r \le +\infty$, and to see what types of temperature behavior one gets for $K_1(T)$, the behavior of $K_2(T)$ being known by Eqs. (21) and (8) and from Fig. 1. However, with just two components $\bar{\kappa}_2$ and $\bar{\kappa}_4$ contributing to $K_1(t)$, it is possible to carry out an ex-

plicit and conclusive analytical classification of the possible types of temperature behavior of $K_1(t)$ *which is valid beyond the MF approximation.* The latter is then applied to corroborate the analytical results and to present graphically their salient features.

In doing so, the central idea has been to examine the signs of the first derivative of $K_1(t)$ at both ends of the interval of variation $0 \leq t \leq 1$, i.e., for $t \to 0$ ($T \to 0$) and $t \to 1^-$ ($T \to T_c^-$) . By Eq. (25), one must then reckon with the derivatives of $\bar{\kappa}_2(t)$ and $\bar{\kappa}_4(t)$, whereby several assumptions and results have to be used. They can be summarized as follows: (i) the (reduced) magnetization per magnetic moment m is a monotonically decreasing function of temperature, so that

$$\frac{\partial m}{\partial t} = T_c \frac{\partial m}{\partial T} < 0 \ , \qquad 0 < t \leq 1 \ ; \tag{33}$$

(ii) the effective field acting on a given moment goes to zero for $t \to 1$; (iii) the $\frac{1}{2}n(n+1)$ law for the variation of $\bar{\kappa}_n$ with magnetization at low temperatures has been evoked:[14]

$$\bar{\kappa}_n \longrightarrow m^{\frac{1}{2}n(n+1)} \qquad \text{for} \qquad t \to 0 \ . \tag{34}$$

Clearly, all these assumptions hold much more generally than in the MF approximation only. The first one is valid beyond any particular model, provided that one examines ferromagnetic interactions between moments on a single magnetic sublattice (at that, this is a sufficient condition only). The second one is just as general as the first when taken conceptually without recourse to any particular ansatz leading to some particular model-dependent self-consistent description of the collective effect of all moments acting on a given moment, i.e., when "effective field" is not restricted to denote "mean field," "molecular field," or the like. The third assumption has been celebrated and generalized ever since 1936 (Refs. 7, 8, 25) as being the result of a purely symmetry argument. The domain of its validity is discussed in Ref. 3 and it is certainly consistent with the assumption of negligible anisotropy in the perpendicular plane.

To carry out the quantitative evaluation of $\partial K_1/\partial t$ in the vicinity of $t = 0$, one needs nothing more than the $\frac{1}{2}n(n+1)$ law. At the other end, $t \to 1$, one needs the explicit expansions of $M_n(x)$ for small x. These can be found from the generating function $\Omega(a,x)$ of the moments M_n (Ref. 15):

$$M_n(x) = \frac{\partial^n}{\partial a^n} \Omega(a,x)_{|a=0}$$

$$= \frac{\partial^n}{\partial a^n} \frac{\sinh[\frac{2S+1}{2}(a+x)]/\sinh[(a+x)/2]}{\sinh(\frac{2S+1}{2}x)/\sinh(x/2)} \ . \tag{35}$$

One finds for $x \to 0$ ($t \to 1$)

$$M_2(x) = \frac{1}{3}J(J+1) + \frac{1}{90}\ J\ (4J^3 + 8J^2 + J - 3)\ x^2, \tag{36}$$

$$M_4(x) = \frac{1}{15}\ J\ (3J^3 + 6J^2 + 2J - 1) + \frac{1}{630}\ J\ (24J^5 + 72J^4 + 34J^3 - 52J^2 - 23J + 15)\ x^2 \tag{37}$$
$$- \frac{1}{37800}\ J(128J^7 + 512J^6 + 696J^5 + 296J^4 - 246J^3 - 388J^2 - 53J + 105)\ x^4 \ ,$$

$$M_6(x) = \frac{1}{21}\ J\ (3J^5 + 9J^4 + 6J^3 - 3J^2 - 2J + 1) \tag{38}$$
$$+ \frac{1}{630}\ J\ (20J^7 + 80J^6 + 65J^5 - 85J^4 - 87J^3 + 61J^2 + 37J - 21)\ x^2$$
$$- \frac{1}{83160}\ J\ (224J^9 + 1120J^8 + 1948J^7 + 1072J^6 - 1075J^5 - 2273J^4 - 519J^3 + 1761J^2 + 577J - 525)\ x^4 \ ,$$

where we have preserved only as many terms as are necessary for the present analysis [the expression for M_6 and the $O(x^4)$ term in M_4 will be needed in the cubic case below]. Carrying out the required calculations, one obtains astonishingly simple results. It turns out that the sign of $\partial K_1/\partial t$ for $t \to 0$ is the same as the sign of the expression

$$S_0 = 8\ K_2^o - 3\ K_1^o \ , \tag{39}$$

while the sign of $\partial K_1/\partial t$ for $t \to 1$ is given by the sign of the expression

$$S_1 = -\left(K_1^o + \frac{8}{7}\ K_2^o\right) \ . \tag{40}$$

The expression in the brackets is the same as in Eq. (25). In fact, the calculation of the first derivative $\partial K_1/\partial t$ for $t \to 1$ with the help of the expressions (36) serves to establish explicitly that a complicated J-dependent polynomial which multiplies S_1 is positive for all physically relevant values of J, so that the sign of $\partial K_1/\partial t$ is ultimately determined by (coincides with) the sign of S_1. The algebra involved should not disguise the persistence and importance of the simple expression $K_1^o + \frac{8}{7}K_2^o$ which originates from a purely symmetry transformation between two equivalent representations of the anisotropy free energy;[23] this suggests that the sign of $\partial K_1/\partial t$ is determined by S_1 beyond any particular theory or class of theories. Hence the whole argument based on the examination of the signs of the above expressions should be expected to be quite generally valid.

The classification of *possible types* of temperature de-

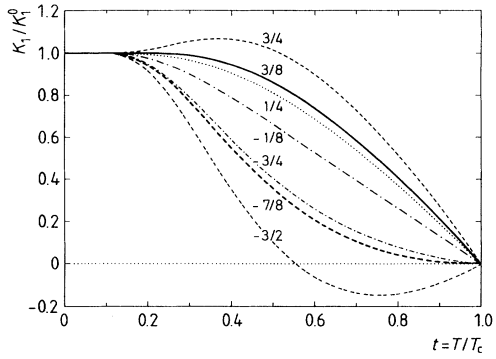

FIG. 2. Uniaxial case with $J = 5/2$. The anisotropy constant $K_1(t)$ as normalized against its zero-temperature value K_1^o in the MF approximation for some typifying ratios of $r = K_2^o/K_1^o$. The value of r is given next to each curve.

pendence of $K_1(T)$ is therefore reduced to considering simultaneously a simple system of inequalities and consecutively examining all possible combinations of signs. Already here, one can see that there are at most four possibilities (two times two combinations of plus and minus signs of S_0 and S_1). In fact, only three of them are allowed for a given sign of K_1^o. The results, illustrated in Fig. 2, can be described as follows.

For positive $K_1^o > 0$, one finds the following.

(a) For $\frac{3}{8}K_1^o < K_2^o$, S_0 is positive, while S_1 is negative implying that $K_1(T)$ *increases* upon increasing the temperature from $T = 0$ and that, furthermore, $K_1(T)$ has at least one local extremum between $T = 0$ and T_c on continuity grounds for its first derivative.

(b) For $-\frac{7}{8}K_1^o \leq K_2^o \leq \frac{3}{8}K_1^o$, both S_o and S_1 are negative. This corresponds to the usual expectations of a monotonically decreasing anisotropy constant from the positive value of K_1^o at $T = 0$ to zero at T_c.

(c) For $K_2^o < -\frac{7}{8}\ K_1^o < 0$, S_0 is negative, while S_1 is positive. Hence $K_1(T)$ must have at least one local extremum between zero and T_c.

Since the linear combination for $K_1(T)$ from Eq. (15) involves two strictly monotonically decreasing functions only, there is no ambiguity with the number and character of the extrema. One has namely a single positive maximum, no extremum (strictly monotonic decrease), and a single negative minimum which goes together with a *change of sign* of the anisotropy constant for the cases (a)–(c) above, respectively.

To avoid superfluous repetition and with the understanding that there exists mirror symmetry of the anisotropy curves $K_1(T)$ with respect to the temperature axis upon changing the sign of K_1^o, the three types per sign of K_1^o can be summarized in terms of the parameter $r = K_2^o/K_1^o$, as follows:

$$\text{Type 1:} \quad r > 3/8 \ ; \tag{41}$$

$$\text{Type 2:} \quad -7/8 \leq r \leq 3/8 \ ; \tag{42}$$

$$\text{Type 3:} \quad r < -7/8 \ . \tag{43}$$

It is very instructive and informative as regards the generality of the conditions derived in Eq. (41) to see how the last condition emerges as a *necessary* condition by building on the most pronounced experimental feature of the corresponding regime, namely, the change of sign of $K_1(T)$ at some temperature $T_S < T_c$. By Eq. (25), the fact of change of sign is formalized by requiring that $K_1(T)$ be zero for T_S, i.e.,

$$\left(K_1^o + \frac{8}{7}K_2^o\right)\bar{\kappa}_2(T_S) - \frac{8}{7}K_2^o\bar{\kappa}_4(T_S) = 0 \ . \tag{44}$$

This is easily transformed to

$$\frac{8}{7}\frac{r}{1+\frac{8}{7}r} = \frac{\bar{\kappa}_2(T_S)}{\bar{\kappa}_4(T_S)} > 0 \ . \tag{45}$$

The positivity requirement which stems from the definition of the basis functions $\bar{\kappa}_n(T)$ can be met by either $r > 0$ or $r < -7/8$. Only the latter is also sufficient as already proved above by the investigation of the signs of the derivative of $K_1(T)$.

Before we give some representative curves for $K_1(T)$ calculated in the MF approximation, it must be emphasized that within the formalism of Refs. 19 and 20, one can compute without difficulty the dependence $K_1(m)$, whereby the temperature dependence can be obtained for every particular material by using the temperature dependence of the magnetization $m(T)$ as measured in *experiments* on the same material.[12] Thus one can avoid discrepancies which might arise when the MF temperature dependence $m(T)$ as calculated *theoretically* for the same substance is introduced into $K_1[m(T)]$. Results along this line will be reported separately. Here we proceed with the calculation of the $K_1(T)$ dependences in the MF approximation for the regimes specified by the inequalities [(41)–(43)]. To this end, the parametric approach introduced in Ref. 24 and improved in Refs. 19 and 20 is applied. In brief, its salient features are that all interesting quantities $\bar{\kappa}_2$, $\bar{\kappa}_4$, K_1, and K_2 are explicitly expressed as functions of the generalized effective field x from Eq. (11). On the other hand the temperature variable t is also parametrized by x. Computing the functions $\bar{\kappa}$ and K *and* t as functions of x, one collects pairs of points computed with the same value of x and plots or tabulates the interesting temperature dependences [$K_1(T)$ in this case]. The values of K_1^o and K_2^o enter as input (experimental) parameters and set the scale and sign of the temperature dependences. Noting once again that it is only the *ratio* of K_1^o and K_2^o that matters in the case of two-constant anisotropy energy F_A' we will not pursue specific cases and values, but will rather choose values for these two parameters that typify a given case without specifying the units of energy per volume which is otherwise the dimensionality of K_i.

The results for $K_1(T)$ are given in Fig. 2. There are *three possible generic scenarios for each sign of* K_1^o. For the sake of brevity, however, we give the plots for $K_1(T)/K_1^o$, thus avoiding the presentation of curves which are mirror reflections of each other for the same $|K_1^o|$ but with opposite signs. The borderlines between the different regimes as specified by the inequalities (41)

are drawn with thick lines. Several curves are given inside each of the three possible scenarios for the temperature behavior of $K_1(T)/K_1^o$. One is thus able to discover a further interesting feature in the "normal," strictly monotonic case: there is a range of positive values of r where the temperature dependence of $K_1(T)$ is *convex upwards* over the whole interval and is in this sense dominated by the temperature behavior of $\bar{\kappa}_2(T)$ which has the same property.[19] This type of curve has been recorded experimentally. Two early examples are the hexagonal ferrite $Ba_2Co_2Fe_{12}O_{22}$ known also as Co_2Y (Ref. 26) and Tb (Ref. 17) (in the latter case, the tail for $T \to T_c$ is due to the applied external field, because the measured quantity was the corresponding magnetostriction constant; cf. Fig. 1.2.2 in Ref. 3). The range of persistence of such behavior can also be determined for the general Callen and Shtrikman class of theories if the *second* derivative of $K_1(T)$ is considered along the lines of the previous section. This means that one can determine a number r_i such that, for $r_i < r < \frac{3}{8}$, $K_1(T)/K_1^o$ is convex upwards for all temperatures below T_c. The value of r_i is certainly negative, because with $r = 0$, K_2^o would be zero which means that one remains with $K_1(T) \sim \bar{\kappa}_2(T)$ and, hence, with a convex-upwards function of T. Even without analytic calculations based on the examination of the second derivative, one can probe, with the help of the parametric approach, different values of r and determine to a very good approximation the value of r_i, above which $K_1(T)/K_1^o$ is convex upwards and below which it has an inflexion point. We find that this value is $r_i \approx -1/8$. It marks the splitting-up into two subdomains of the domain $-7/8 \leq r \leq 3/8$, hence, the subscript i in r_i stands for "internal" borderline. More precisely, for $-7/8 \leq r < -1/8$ one has the "usual" temperature behavior of $K_1(T)/K_1^o$ with an inflexion point, while for $-1/8 < r \leq 3/8$ one finds a convex-upwards regime. One comes to the important conclusion that in uniaxial symmetry the "normal," monotonically decreasing bell-shaped dependence for $K_1(T)$ with an inflexion point can only be realized if the intrinsic constants K_1^o and K_2^o are of different signs, i.e., it is necessary that r be negative. The ratio inflexion to convex as measured by the size of the corresponding domains in r is 3:2 which means that the range of values of r for which the convex-upwards behavior may be observed is almost as large as the "usual" one. In Fig. 2, the *inner borderline curve* for the regime specified by the relation (42) is the fourth from above or below ($r = -1/8$). Apart from its role of an inner dividing line inside the generic regime of strictly monotonic decrease of $K_1(T)/K_1^o$, it is interesting in itself, since it can be approximated quite well with two straight pieces: a horizontal part stretching from $T = 0$ to $T \approx 0.2T_c$ and a part of *linear decrease* from $T \approx 0.2T_c$ to T_c.

The whole procedure of dealing with this important feature of the temperature behavior of $K_1(T)$ inside the regime defined by the second inequality in Eq. (41) emphasizes the indispensability of the parametric approach in probing the different regimes.

In both cases of positive or negative K_1^o the temperature dependence of $K_2(T)$ is given, up to scale and sign of

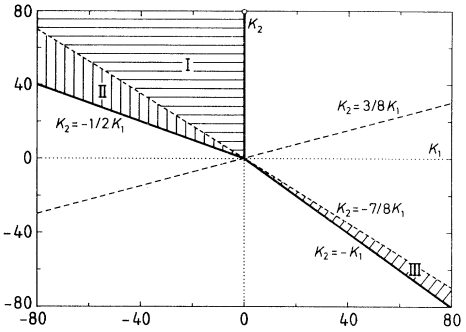

FIG. 3. Thermodynamically stable phases with uniaxial anisotropy: (i) easy-axis phase: $K_1 > 0, K_2 > -K_1$; (ii) tilted-axis phase: $K_1 < 0, K_2 > -K_1/2$; (iii) easy-plane phase: the rest of the (K_1, K_2) plane. Thick lines are borderlines between different thermodynamic phases, while dashed lines represent borderlines between regimes with different types of temperature dependence of $K_1(T)$. Systems starting their temperature evolution at $T = 0$ in one of the wedges I, II, or III would cross over to a more stable phase at a certain spin-reorientation temperature $T_S < T_c$ (see text and Fig. 4). Systems evolving from any other point would not change their thermodynamically preferred phase.

K_2^o, by the corresponding dependence of $\bar{\kappa}_4(T)$ (cf. Fig. 1).

It is not by chance that we keep recalling about $K_2(T)$ as well. It is the *set of both constants* K_1 *and* K_2 that determine in a standard thermodynamical procedure the equilibrium directions (the easy axes) of magnetization. In Fig. 3 we reproduce the well-known phase diagram for easy-axis directions when the uniaxial anisotropy energy is given by Eq. (20); the thick lines are the borders between the three thermodynamically allowed phases. The three possibilities are that the easy axis is (i) along the z axis, (ii) in the plane perpendicular to the z axis, or (iii) tilted under an angle θ with respect to the z axis so that $\sin^2\theta = -K_1/2K_2$. This picture is static in the sense that for a given temperature, say T_1, $K_1(T_1)$ and $K_2(T_1)$ have definite values which determine a point in the plane (K_1, K_2). Suppose now that at $T = 0$ the system is specified by the point (K_1^o, K_2^o) in the phase diagram of Fig. 3. As both anisotropy constants change with temperature quite differently (cf. Figs. 1 and 2), by increasing the temperature from $T = 0$ to T_c the system will be forced to evolve along a specific trajectory $[K_1(T), K_2(T)]$ parametrized physically by the temperature T. All possible trajectories flow into the origin at $T = T_c$ since both one-ion anisotropy constants are zero in zero external field. It is then quite possible that, at some value of temperature which depends on the initial conditions at zero temperature, this trajectory crosses over to some neighboring domain. Accordingly, at this particular temperature the easy axis must switch to the new easy direction. Such behavior has been observed in many uniaxial materials and notably in $Nd_2Fe_{14}B$.[27–29] Furthermore, whenever the temperature evolution of the anisotropy constants (i.e., the anisotropy trajectory as

described above) is such that the uniaxial system starts from the tilted-axis domain of Fig. 3 over some temperature range, *the temperature evolution of the angle θ can also be described within the same formalism.* Following the analysis of the preceding sections, we are now in the position to describe and predict such crossovers and peculiarities in great detail. The initial condition (K_1^o, K_2^o) is of exceptional importance. Given this pair, the temperature flow of the anisotropy is deterministic within the discussed theory.

Following the introduced systematics, we give the temperature evolution of the anisotropy constants assuming initial conditions which lead in turn to one of the generic types of behavior of $K_1(T)$ described above. The generation of the corresponding trajectories is effectuated within the parametric approach of Refs. 19, 20, and 24 as outlined above. One need only make a minor effort and collect pairs of points (K_1, K_2) which have already been calculated in the parametric sweep of x necessary for the computation of K_1 and K_2. A brief thought leads to a very important observation: *physically*, it is the temperature that drives the flow of the anisotropy constants in the plane (K_1, K_2); however, in our approach the temperature itself is parametrized by the generalized effective field x of Eq. (11); therefore, by generating the anisotropy flows we are practically using the parametrization $[K_1(x), K_2(x)]$. In this way one avoids the necessity to use the MF expression connecting temperature t and effective field x which means that *the trajectories in the plane (K_1, K_2) given below are valid for the whole class of untrivial collective-excitation theories.*[15] Note once again the great potential power of the parametric approach.

Illustrative results are given in Fig. 4 for all typical initial conditions. Theoretical flow diagrams for the anisotropy corresponding to the three generic regimes given in Fig. 2 are being presented.

We begin the scrutiny of the anisotropy flow diagrams by the general remark that in the two-constant case for the anisotropy energy as given in Eq. (20) the anisotropy constant K_2 evolves upon variation of temperature without changing its sign [cf. the first Eq. (21)]. Therefore, a flow starting in the upper $(K_2 > 0)$ or lower $(K_2 < 0)$ half-plane will not leave it. Whenever a trajectory crosses one of the phase lines as given in Fig. 3 and reproduced in Fig. 4, the system runs away to another thermodynamic phase. The analysis indicates that three distinct crossovers may take place: cone-to-axis, cone-to-plane, and axis-to-plane. The crossovers are unique (there are no successive crossovers to other easy axes or backward crossovers) and take place at a certain spin-reorientation temperature T_S. The existence and the type of crossover are determined *solely by the initial conditions, i.e., the values of K_1^o and K_2^o.* Thus there are three wedges in the phase diagram (K_1, K_2) (I, II, and III in Fig. 3) which correspond to the three distinct crossovers. Two of the wedges are in the second quadrant and one is in the fourth quadrant. It is clear that there is no symmetry with respect to the sign of K_1^o when the temperature evolution of the anisotropy is concerned. This emphasizes once again the necessity to treat with care the signs of the zero-temperature values K_1^o and K_2^o. The wedges

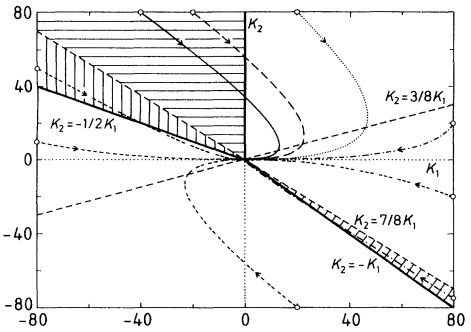

FIG. 4. Anisotropy flow diagrams in the (K_1, K_2) plane for the uniaxial case with $J = 5/2$. Thick lines are borders between the three thermodynamically stable phases; dashed straight lines come from the analysis of the types of temperature dependence of K_1 (Fig. 3). The representative initial conditions (K_1^o, K_2^o) can be read off the coordinates of the empty dots. The arrows indicate the direction of temperature evolution as T increases from zero to T_c. The point where a given trajectory crosses a thick line corresponds to the spin reorientation at a temperature $T_S < T_c$ (cf. Fig. 5).

are now named by the type of crossover to which they lead on increasing the temperature and are defined as follows:

(i) the cone-to-axis wedge I (second quadrant):

$$-\frac{7}{8}K_1^o < K_2^o, \qquad K_1^o < 0\ ; \tag{46}$$

(ii) the cone-to-plane wedge II (second quadrant):

$$-\frac{1}{2}K_1^o \le K_2^o \le -\frac{7}{8}K_1^o, \qquad K_1^o < 0\ ; \tag{47}$$

(iii) the axis-to-plane wedge III (fourth quadrant):

$$-K_1^o < K_2^o < -\frac{7}{8}K_1^o\ , \qquad K_1^o > 0\ . \tag{48}$$

It is thus clear that the different phases as defined by thermodynamic minimization (Fig. 3) are of different relative stability under variation of temperature. The tilted-axis phase $(K_1 < 0, K_2 > -\frac{1}{2}K_1$ in Fig. 3) is the most unstable in the sense that systems starting their temperature evolution from within this phase run away to either of both neighboring phases. The c-axis phase is of intermediate stability; in fact, up to the existence of the thin wedge III, the systems starting from within this phase remain within. The easy-plane phase is the most stable in this sense and a system starting at $T = 0$ from within never leaves it. This is exactly the picture one observes in rare-earth–transition-metal–boron compounds.[27,29] Further quantitative analysis of this correspondence will be given elsewhere.

So far as the temperature T_S of the corresponding crossover is concerned, the plots K_2 versus K_1 are only indicator plots. However, establishing with their help the *existence* of a crossover between preferred directions, one

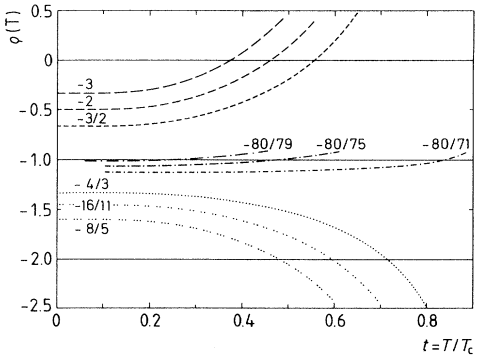

FIG. 5. Uniaxial case with $J = 5/2$: $\rho(t) = K_1/K_2$ in the MF approximation. The thick horizontal lines $\rho_{\rm cross} = 0, -1, -2$ are the thick borderlines of Figs. 3 and 4 in the representation $\rho = \rho(t)$; crossing these lines corresponds to cone-to-axis, axis-to-plane, and cone-to-plane crossovers, respectively, while the crosspoints give T_S in the MF approximation. For each type of crossover three representative curves with different ratios r from within the corresponding crossover-inducing wedges are given; from above: (i) cone-to-axis (wedge II); (ii) axis-to-plane (wedge III); (iii) cone-to-plane (wedge I). The relevant values of r are given in the plot.

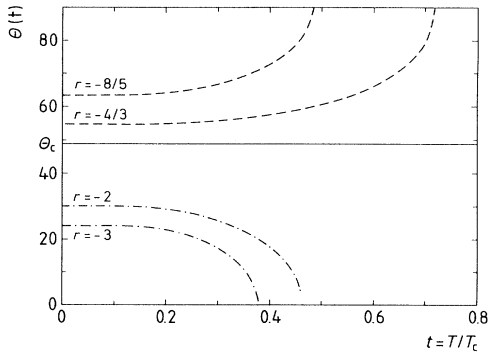

FIG. 6. Uniaxial case ($J = 5/2$). Temperature dependence of the cone angle $\theta(t)$ in the MF approximation. From above: cone-to-plane crossover (wedge I); cone-to-axis crossover (wedge II).

may proceed and determine this crossover temperature. The answer is readily found by using the parametric approach and plotting the ratio

$$\rho(T) = \frac{K_1(T)}{K_2(T)} \ . \tag{49}$$

In Fig. 5, we give $\rho(T)$ for some representative cases for which one detects a crossover. From the intersections of $\rho(T)$ with the lines of crossover $\rho_{\rm cross} = -2, -1, 0$, respectively, one is able to determine unambiguously T_S for the corresponding crossover. There is a clearly expressed correlation between the width of the three crossover-inducing wedges and the sensitivity of the crossover temperature T_S: the narrower a wedge is as measured by the corresponding value of the dimensionless parameter r of Eq. (41), the more sensitive the spin-reorientation temperature T_S to changes of these parameters within the given wedge and, correspondingly, the wider the *spread* of T_S on changing r. For example, varying the ratio of K_2^o and K_1^o by about 10% for the narrowest axis-to-plane wedge [Eq. (48)] brings about a threefold change in T_S, while varying the said ratio by a factor of 2 within the widest cone-to-axis wedge [Eq. (46)] initiates "only" a 1.5-times variation in the corresponding values of T_S (cf. Fig. 5).

Finally, in Fig. 6 we give the temperature dependence of the cone angle $\theta(T)$ for some representative cases from the previous plots where the system's anisotropy sets off along its temperature-variation trajectory from within a wedge corresponding to a domain of a tilted-axis phase at $T = 0$, i.e., from one of the two wedges in the second quadrant [inequalities (46) and (47)]. While the analytic form of the curves $\theta(T)$ is the same in both cases and is given by

$$\theta(T) = \arcsin\left[-\frac{K_1(T)}{2K_2(T)}\right]^{1/2} \ , \tag{50}$$

their appearance depends on the detailed temperature variation of both anisotropy constants. From Eq. (50) one can determine a critical angle

$$\theta_{\rm cr} = \theta(T = 0, |r| = 7/8) = \arcsin(4/7)^{1/2} = 49.1^\circ \ , \tag{51}$$

such that for the cone-to-axis inducing wedge we have $\theta \in [0, \theta_{\rm cr}]$, while for the cone-to-plane inducing wedge the angle θ is restricted to the domain $[\theta_{\rm cr}, \pi/2]$. From another point of view, already a single measurement of the cone angle at any temperature for which the system is in the tilted-axis phase indicates to which part (or wedge) within this phase in the second quadrant the system belongs. Reversing the argument, one can deduce the ratio r from a single measurement at a sufficiently low ($T \to 0$) temperature, provided that there are no other contributions to the anisotropy energy or that they have already been subtracted.

The thermodynamic analysis of the uniaxial case is thus complete.

B. Cubic symmetry

Now we shall present as concisely as possible the *cubic* case. The details being explained on the example of the uniaxial system, only the most important considerations and results will be mentioned.

1. The one-parameter cubic case

This is when only the term with K_1 in the phenomenological expression (16) is kept. By Eqs. (17),

$$K_1(T) = a_1 \bar{\kappa}_4(T) = K_1^o \bar{\kappa}_4(T) \ . \tag{52}$$

Following the analysis of the previous sections, this expression characterizes exhaustively the one-ion anisotropy in cubic symmetry for $J = 2$ and $J = 5/2$. It would be a reasonable approximation for higher J as well, if the constants $|K_i(i > 1)| \ll |K_1|$. The scale and sign of K_1 are set by the zero-temperature value K_1^o, while the temperature dependence is that of $\bar{\kappa}_4(T)$. This has been shown to have the characteristic bell shape in both the MF and in the RPA with an inflection point as discussed above (Fig. 1). Note that here a calculation in an untrivial collective-excitation scheme giving the correct spin-wave result at low temperatures is available.[20] To do this, a more elaborated version of the parametric approach was developed and explicit expressions for the number of magnons in all cubic lattices have been found by computing the relevant Bose-Einstein lattice sums.[30] This means that the general thermodynamic analysis of possible types of temperature dependence of anisotropy constants in cubic materials can be carried out to the end beyond the MF approximation.

Just like in the uniaxial case, the arguments leading to the description of the various general types of possible temperature behavior of magnetic anisotropy of single-ion origin suggest validity beyond that characteristic of any given member of the Callen and Shtrikman class. Besides, so far as the explicit temperature dependence is concerned we prefer to treat the cubic case on equal footing with the uniaxial one, i.e., in the MF approximation. Apart from the "homogeneity-of-treatment" considerations, we feel that (i) it is always recommendable to start the description with the MF approximation which has proven to give sound physical insights into the nature of the examined problems, (ii) it will be possible to compare both cases on the higher (RPA) level once current calculations of the required lattice sums in uniaxial symmetry are brought to an applicable form, and (iii) an even more promising collective-excitations scheme which implements the Callen decoupling scheme[31] could also be applied. Remarking that the calculations can be performed equally easily for any J, in Fig. 7 we give in the MF approximation only the curves $\bar{\kappa}_4(T)$ and $\bar{\kappa}_6(T)$ for $J = 3$ and $J = 7/2$ which will be needed in the two-parameter case. Note that the temperature dependence of $\bar{\kappa}_6(T)$ in the MF approximation has not to our knowledge been reported previously in the literature.

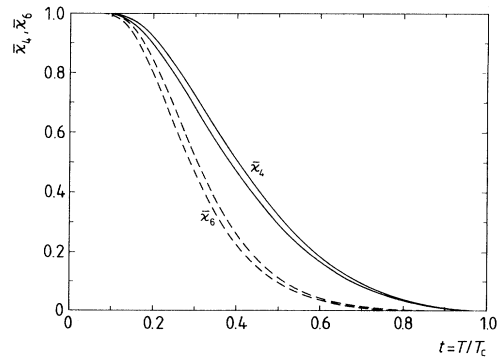

FIG. 7. Magnetic anisotropy coefficients $\bar{\kappa}_4$ and $\bar{\kappa}_6$ as functions of reduced temperature $t = T/T_c$ for $J = 3$ and $7/2$ in the MF approximation. Within each pair of curves the upper one is for smaller J. Both coefficients have a typical bell shape with $\bar{\kappa}_6$ falling off much faster.

2. *The two-parameter cubic case*

This is when two anisotropy constants are considered in the expression (17). The relevant anisotropy is now given by Eq. (16), where

$$K_1(T) = \left(K_1^o + \frac{1}{11} K_2^o\right)\bar{\kappa}_4(T) - \frac{1}{11} K_2^o \bar{\kappa}_6(T) \; ; \quad (53)$$

$$K_2(T) = K_2^o \bar{\kappa}_6(T) \; . \quad (54)$$

The anisotropy energy as given by Eq. (16) is exhaustive for $J = 3$ and $J = 7/2$ and can be taken as a good approximation even for $J > 7/2$ if there are reasons to assume that $|K_i(i \geq 3)| \ll |K_1|, |K_2|$. More significantly and as commented earlier, for a rare-earth ion sitting in a (local) cubic environment the two-parameter expression for $F_A^{c\prime}$ is *exhaustive* for any value of J.

Working along the lines of the "uniaxial" section, one finds that the signs of $\partial K_1(T)/\partial T$ at both ends of the temperature interval $(0, T_c)$ are determined by (coincide with) the signs of the following expressions:

$$\begin{aligned} T \to 0: \quad & S_o^c = K_2^o - 10K_1^o \; , \\ T \to T_c: \quad & S_1^c = -(K_1^o + \tfrac{1}{11}K_2^o) \; . \end{aligned} \quad (55)$$

Here the superscript c stands for "cubic." In the above expression for S_o^c, the coefficient of 10 originates from the $\frac{1}{2}n(n+1)$ law. The expression in the brackets of the equation for S_1^c is the one from Eq. (53). Straightforward algebra using the asymptotic ($t \to 1$) expansions of the moments $M_n(x)$ [Eqs. (36)] produces no less than the explicit proof, within the Callen and Shtrikman class of theories, that a certain complicated J-dependent polynomial which multiplies S_1^c in the expression for $\partial K_1/\partial t(t \to 1)$ is positive for all physically relevant values of J, so that the sign of $\partial K_1/\partial t(t \to 1)$ is ultimately determined by the sign of S_1^c as stated above.

As before, the *possible types of temperature dependence* of $K_1(T)$ are determined by considering simultaneously the corresponding simple system of inequalities involving all possible signs of S_o^c and S_1^c. Once again, three generic types per sign of K_1^o are allowed.

For positive $K_1^o > 0$, one finds the following.

(a) For $10K_1^o < K_2^o$, S_o^c is positive, while S_1^c is negative. $K_1(T)$ *increases* from its positive zero-temperature value, passes through a positive maximum, and falls off to zero at T_c.

(b) For $-11K_1^o \leq K_2^o \leq 10K_1^o$, both S_0^c and S_1^c are negative. $K_1(T)$ decreases strictly monotonically from K_1^o at $T = 0$ to zero as $T \to T_c$. For all values of this interval, which is much larger than the corresponding interval in the uniaxial case, one finds the characteristic bell shape of $K_1(T)$. There is no range of values of K_2^o for which $K_1(T)$ is convex upwards over the entire range $[0, T_c]$. This difference from the corresponding uniaxial

case arises because none of the basis functions $\bar{\kappa}_4(T)$ and $\bar{\kappa}_6(T)$ is convex upwards over the whole range, contrary to $\bar{\kappa}_2(T)$ in the uniaxial case.

(c) For $K_2^o < -11K_1^o$, S_0^c is negative, while S_1^c is positive. $K_1(T)$ decreases, changes sign at some $T_S < T_c$, passes through a negative minimum, and goes to zero from the negative side.

The three cases with negative K_1^o follow by recalling the reflection symmetry of the anisotropy curves with respect to the temperature axis upon changing the sign of K_1^o.

In terms of the parameter $r = K_2^o/K_1^o$, the respective types are compactified to

$$\text{Type 1:} \quad r > 10 \; ; \tag{56}$$

$$\text{Type 2:} \quad -11 \leq r \leq 10 \; ; \tag{57}$$

$$\text{Type 3:} \quad r < -11 \; . \tag{58}$$

An important conclusion based on the above general inequalities is that the two outermost types could hardly be realized in practice, since they require that $|K_2^o|$ be more than an order of magnitude greater than $|K_1^o|$ and this seems rather improbable, although it cannot be ruled out by general arguments. Therefore, while one is in his right to expect, theoretically, three generic types of temperature behavior for each possible sign of K_1^o, in cubic symmetry it seems more realistic to expect to detect only one generic type per sign of K_1^o. Now one is in the position to explain the paradigm confirmed in many experimental studies of magnetic anisotropy and magnetostriction[32] that the single-ion anisotropy constant $K_1(T)$ in cubic symmetry should be a bell-shaped, monotonically decreasing curve. The compact inequality

$$-11 \leq r \leq 10 \qquad (r = K_2^o/K_1^o) \tag{59}$$

which comprises both possible signs of K_1^o and K_2^o *defines the limits of validity* of this built-in belief. The issue is further illuminated in Fig. 8. There, the lowest and the highest curves are typical for the outermost generic regimes and it should be noted what large ratios $|K_2^o/K_1^o|$ are involved in each of these theoretically possible generic cases. The interior between the thick borderline curves in both figures is the regime described by the inequality (59). One must realize that changing the ratio $|K_2^o/K_1^o|$ by more than an order of magnitude in both the positive and the negative direction of values of K_2^o induces but relatively small variation in the $K_1(T)$ curves within the interior of the domain specified by the inequality (59). Moreover, in order to feel more clearly what is going on with the $K_1(T)$ dependence upon variation of the K_2^o value in cubic symmetry, we have given in the same figure the curves corresponding to variation of K_2^o between $(-K_1^o)$ and $(+K_1^o)$, i.e., for

$$-1 \leq r \leq 1 \; . \tag{60}$$

In Fig. 8, the corresponding domain comprises just the narrow region bounded by the innermost pair of curves. In other words, nothing much is happening qualitatively *and* quantitatively within a range of values of K_2^o as wide as $2|K_1^o|$.

As before with the uniaxial case, all curves are generated with the help of the parametric approach as described in Refs. 19, 20, and 24. We recall once again that only the curves which involve an explicit temperature dependence make use of the MF approximation. Now that we proceed with the analysis of the anisotropy flows in the (K_1, K_2) plane, it should be emphasized that all conclusions reached by analysis of these flows in the said plane are valid beyond the MF approximation. As before, it is the *set of both constants* K_1 *and* K_2 that determine the equilibrium directions (easy axes) of magnetization. The well-known diagram for the thermodynamically preferred directions of magnetization as described by the two-constant phenomenological expression $F_A^{c\prime}$ is repro-

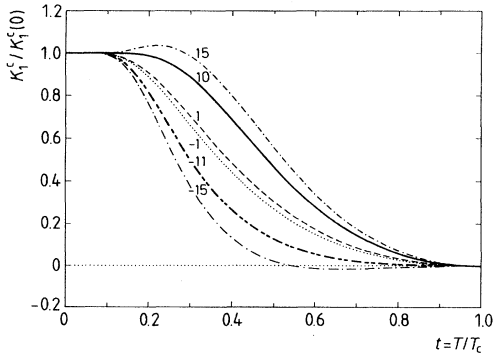

FIG. 8. Cubic symmetry with $J = 7/2$ in the MF approximation. $K_1^c(t)$ as normalized against $K_1^c(0)$ for typifying ratios of r (given in the plot). Thick lines are borderlines between different temperature scenarios (see text). K_i are superscribed with c for "cubic" only in the figures, not in text.

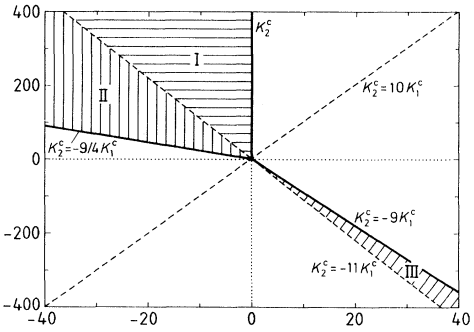

FIG. 9. Thermodynamic stability for cubic anisotropy: easy axis along (i) an edge of the cubic cell $(K_1^c > 0, K_2^c > -9K_1^c)$; (ii) a face diagonal $(K_1^c < 0, K_2^c > -\frac{9}{4}K_1^c)$; (iii) a body diagonal (the rest of $K_1^c - K_2^c$ plane). Thick lines are borders between these thermodynamic phases, while dashed lines represent borderlines between regimes with different types of temperature dependence of $K_1(T)$. The wedges I, II, and III induce a crossover to a neighboring phase whenever the temperature evolution starts from within them at $T = 0$.

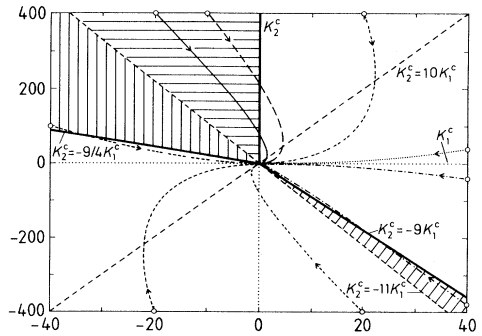

FIG. 10. Anisotropy flow diagrams for the cubic case with $J = 7/2$. Borderlines of phases and crossover-inducing wedges are as in Fig. 9. Arrows mark the direction of the temperature evolution.

duced in Fig. 9. In the same figure we give for the first time the borderlines between the different regimes as defined by the joint examination of the possible signs of S_o^c and S_1^c.

Now there are three thermodynamically allowed easy-axis directions: (i) along the edge, (ii) along the body diagonal, and (iii) along the diagonal of a face of the cubic cell. Contrary to the uniaxial case, within none of the three phases may the easy axis change its direction continuously.

The general discussion concerning the temperature-driven flow of the system in the (K_1, K_2) plane proceeds as for the uniaxial case. In Fig. 10 we give the anisotropy flow for cubic systems. The results are valid for the whole class of theories of Callen and Shtrikman,[15] at least. Representative values (K_1^o, K_2^o) have been chosen. As before, a flow which starts in the upper $(K_2^o > 0)$ or lower $(K_2^o < 0)$ half-plane will not leave it. Whenever a trajectory crosses one of the phase lines, the easy axis switches to another direction. Note that, in contrast to the crossovers from the tilted-axis phase in the uniaxial case where the direction in fact slides continuously to the easy crystallographic axis or plane of the neighboring thermodynamic phase, in the cubic case one has an abrupt switching to another direction when the trajectory crosses a phase border. This issue can be further analyzed by means of the theory of first-order magnetic processes[33,34] which is also the relevant theory if the influence of an externally applied magnetic field is to be studied. The analysis indicates that only three distinct crossovers may take place: $\langle 110\rangle$ to $\langle 100\rangle$, $\langle 110\rangle$ to $\langle 111\rangle$, and $\langle 111\rangle$ to $\langle 100\rangle$ (here the brackets denote the corresponding crystallographic directions). The crossovers are unique and take place at a certain spin-reorientation temperature T_S. The existence and the type of crossover are determined *solely by the initial conditions, i.e., the values of* K_1^o *and* K_2^o. Thus one identifies three wedges in the phase diagram (K_1, K_2) (I, II, and III in Fig. 9) which lead to three distinct crossovers. The wedges are defined by the inequalities:

(i) wedge I (second quadrant):

$$-11K_1^o < K_2^o, \qquad K_1^o < 0\ ; \tag{61}$$

(ii) wedge II (second quadrant):

$$-\frac{9}{4}K_1^o < K_2^o < -11K_1^o, \qquad K_1^o < 0\ ; \tag{62}$$

(iii) wedge III (fourth quadrant):

$$-11K_1^o < K_2^o < -9K_1^o\ , \qquad K_1 > 0\ . \tag{63}$$

It is thus clear that the phase with an easy axis along the plane diagonal is unstable under the temperature evolution of the cubic anisotropic system: the temperature flow trajectories will always leave the corresponding part of the phase diagram and cross over to the neighboring more stable phases with easy axes along the edge or the body diagonal. On the other hand, the phase with an easy axis along the edge is the most stable one in the sense that, if a system belongs there at $T = 0$, it will remain there under the temperature evolution of anisotropy, i.e., the easy axis will not change its direction over the entire range between 0 and T_c. The phase with an easy axis along the body diagonal has marginal stability in the above sense: up to the existence of the very thin wedge III, a system which has been within the domain at $T = 0$ will evolve without crossing over to a phase with some other easy axis; for systems represented by points from within the wedge III there will occur a crossover to the easy-edge phase at some temperature.

As in the uniaxial case, once the existence of a crossover for a given system as specified by its initial point (K_1^o, K_2^o) has been established, one may proceed and determine the crossover temperature with the help of the parametric approach. As mentioned earlier, for cubic systems one may go beyond the MF temperature dependences of the various interesting quantities [here $\rho(T) = K_2/K_1$].[20,30] We prefer, however, to give only the MF curves at this stage. In Fig. 11, we give $\rho(T)$ for some representative cases of runaway from the most unstable phase $\langle 110\rangle$ to its phase-diagram neighbors $\langle 100\rangle$ and $\langle 111\rangle$. The third possible runaway from $\langle 111\rangle$ to

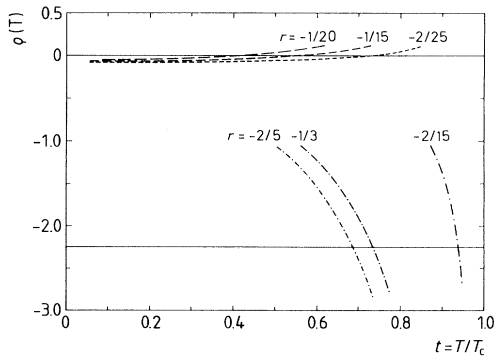

FIG. 11. Cubic case with $J = 7/2$: $\rho(t) = K_1^c/K_2^c$ in the MF approximation. The thick horizontal lines $\rho_{\text{cross}}^{\text{I,II}} = 0; -9/4$ are the thick borderlines between the $\langle 110\rangle$ phase and its neighbors from Figs. 9 and 10. Upper crossover: $\langle 110\rangle$ to $\langle 100\rangle$; lower crossover: $\langle 110\rangle$ to $\langle 111\rangle$. The cross-points of the $\rho(t)$ curves with the dotted borderlines give the corresponding T_S.

$\langle 100 \rangle$ has not been presented in the same figure for reasons of discernibility only; it is just as easily treated as those given in the figure. From the intersections of $\rho(T)$ with the critical lines of crossover $\rho_{\text{cross}} = -2\frac{1}{4}, -\frac{1}{11}, 0$, one is able to determine unambiguously T_S. The correlation between the width of the crossover-inducing wedges and the sensitivity of T_S to the initial ratio r at $T = 0$ is as follows: the narrower a wedge is, the more sensitive the spin-reorientation temperature T_S to changes of the ratio r within the given wedge and, correspondingly, the wider the *spread* of T_S. For example, varying the ratio of K_2^o and K_1^o by about 15% for the narrowest wedge III [Eq. (63)] brings about a threefold change in T_S [not given in Fig. 11], while varying the said ratio within the other two wedges is not so drastic in its effect on T_S.

The thermodynamic analysis of the cubic case is thus complete, too.

VI. PROSPECTIVE GENERALIZATIONS AND APPLICATIONS OF THE GENERAL ANALYSIS

A. Analyses of cases of particular interest

The temperature dependence of $Nd_2Fe_{14}B$ can be reanalyzed in view of the present development and on the basis of the by now well-established picture, the two-sublattice model, for the hierarchy of interactions between magnetic rare-earth and transition-metal ions which results in the observed high magnetization and magnetic anisotropy in this and related materials.[29,35–38]

The starting and encouraging point is the observation that the ratio of the experimentally measured constants K_2^o and K_1^o ($K_1^o < 0$) is approximately (-3) (Refs. 10 and 28) and falls into the third group from the classification for the uniaxial case above. It is satisfactory to see, by comparing the relevant typifying curve for this case (the lowest curves in Figs. 2 and 6) and the experimental results, that the general analysis is confirmed by the character of the curve $K_1(T)$ in this complex magnetic material. Furthermore, beside the qualitative scenario for $K_1(T)$ one gets qualitatively correct predictions, by *general arguments only*, for the spin-reversal temperature T_S (Fig. 5) and for the temperature dependence of the cone angle $\theta(T)$ (Fig. 6). Note that these reference figures are not generated with the actual values of J and K_i^o for $Nd_2Fe_{14}B$, but are just the characteristic curves for the thermodynamical regime as defined for the corresponding uniaxial type. It is beyond doubt that the careful analysis suggested below would improve the agreement between theory and experiment on a basis which is free from further "convenient" *ad hoc* assumptions.

The necessary steps are as follows. First, the contribution of the Fe sublattice has to be subtracted from the anisotropy constant $K_1(T)$, thus leaving the pure RE contribution. The Fe contribution can be taken from measurements on the isostructural material $Y_2Fe_{14}B$ (Ref. 39) scaled to the critical temperature of its Nd counterpart; there, it is the only anisotropy contribution.[29,39,40]

Second, the estimation of the contribution of the Nd sublattice starts with the assumption that the Nd^{3+} ions have $J = 9/2$ as in their free state. By our analysis, one needs to consider K_i up to $i = 3$.[41] The relevant parameters $\{a; b; \ldots; d\}$ for the triangular transformation between anisotropy constants and anisotropy coefficients being known up to $p = 3$,[28,40] and the zero-temperature constants being carefully measured also up to $p = 3$,[10,28] one possesses the physical input necessary for the implementation of the analysis as outlined in this paper.

Third, care has to be taken to avoid a blind application of the parametric approach discussed above and used for the generation of the typical curves. Namely, the generalized effective field x acting on the RE atoms is not a self-consistent field stemming from the RE-RE exchange which is negligible in this and related materials.[36,42] Within the established MF approximation for the treatment of the RE–transition-metal ion interactions, the zero-field Hamiltonian $\mathcal{H}_0$ is proportional to $\mathbf{J} \cdot \mathbf{H}_{\text{Fe}}$, where $\mathbf{H}_{\text{Fe}}$ is the strong effective magnetic field proportional to the magnetization of the Fe sublattice. The bare Hamiltonian thus having $2J + 1$ relevant levels with $J = 9/2$, the generating function $\Omega(a, x)$, the moments $M_n(x)$, and the normalized anisotropy coefficients $\bar{\kappa}_n(x)$ remain the same functions of x as given earlier in this paper. However, here x is treated as an effectively *external field* acting on the RE ions. The difficulty here is recognized by the fact that, unlike an externally applied magnetic field, this effective field varies with temperature as the magnetization of the Fe sublattice and goes to zero as $T \to T_c$. Since the temperature dependence of $m_{\text{Fe}}(T)$ is assumed known from the duly scaled isostructural measurements and since, furthermore, the transition temperature T_c is one and the same for both sublattices, one must only feed in into the formalism $m_{\text{Fe}}(T)$ as taken from experiment. Alternatively, one can take $m_{\text{Fe}}(T)$ from a theoretical self-consistent calculation within the MF approximation with $J = S = 1$ within the same parametric approach (assuming that the iron sublattice magnetization comes from ions with quenched orbital momentum and effective spin number $S = 1$). In fact, it will be interesting to see how much these two procedures differ as regards the final outcome for the one-ion anisotropy. Besides, even the small contribution from the RE-RE exchange can be accounted for in the effective field x within the parametric approach additively and on equal footing with the dominating contribution from the Fe sublattice as can also be done with an externally applied magnetic field. If this program is carried out to the end, one would have the most detailed analysis of the one-ion contribution to the anisotropy in the series of novel hard magnetic materials typified by $Nd_2Fe_{14}B$. Obviously, the program is not restricted to this material only and even not to this series only.

B. Exact energy levels

Further progress with respect to the accuracy of the theoretical predictions on the basis of the suggested scheme is to be expected if the averages involved in the

statistical-mechanical treatment are taken with the exact spectroscopic or theoretical levels characteristic for each particular material[43] and not necessarily with the equidistant $2J+1$ levels leading to the specific form of the generating function $\Omega(a,x)$. Such nonequidistant averaging would not change the general expressions for K_i and $\bar{\kappa}_n$ as functions of the moments $M_n(x)$ but will complicate the computations and eventually change the values of the moments. These modifications are not very dramatic as has been found in preliminary calculations by the present authors for comparing the present approach with the calculations of Wolf with nonequidistant energy levels.[12] Nevertheless, the utmost objective would be to compute the averages for the moments with the relevant exact energy levels involved in each specific case. On the other hand, the general inequalities derived here for the two-constant case are unlikely to be modified, since they are based on quite general thermodynamic considerations.

VII. SUMMARY

We have determined and systematized from a general viewpoint the possible types of temperature dependence of single-ion anisotropy in uniaxial and cubic ferromagnets. The analysis has been based on the general relation between anisotropy constants K_i and coefficients $\bar{\kappa}_n$, the latter serving as a fundamental basis spanning the temperature dependence of anisotropy free energy. As there are no explicit analytic expressions for the calculation of the interesting anisotropy characteristics, a very powerful parametric approach has been used throughout. This approach has made it possible to trace down the temperature-driven evolution of the anisotropy in any given system whose intrinsic anisotropy constants K_1^o and K_2^o are known. The analysis of the flow diagrams, combined with the parametric method, has enabled us to determine regions in the general anisotropy diagram (K_1, K_2) which lead, upon increasing the temperature from $T = 0$, to the experimentally observable transitions (crossovers) between thermodynamic phases with different easy axes of magnetization. The crossovers themselves as well as the loci of the corresponding spin-reorientation temperature T_S have been determined and presented graphically for a series of typical values of the relevant parameter $r = K_2^o/K_1^o$. Special attention has been given to the temperature evolution of the tilted easy axis in the uniaxial case.

The analysis is the outcome of the first-order statistical-mechanical treatment of one-ion anisotropy. Most of the results are valid for the whole untrivial class of Callen and Shtrikman theories, i.e., beyond the MF theory; only those temperature-flow diagrams which contain explicit temperature dependence (temperature axis, respectively) are bound to the MF theory. For cubic materials, even these can be extended to the RPA scheme, since the necessary analytic basis has already been set up.[19,20] Prototype materials to which the analysis is immediately applicable are those in which the one-ion contribution comes from RE ions such as RE–transition-metal compounds or the RE metals themselves.

In view of the fundamental theory of magnetostriction,[32] most of the conclusions about the temperature dependence of anisotropy reached in this paper are immediately applicable to the characterization of magnetostriction in the corresponding substances.

ACKNOWLEDGMENTS

Y.M. acknowledges with gratitude the financial support of the Alexander von Humboldt Foundation (Bonn) and the hospitality of the Max-Planck-Institut für Metallforschung (Stuttgart); work related to Contract No. Φ205/BSF.

---

* On leave from the Institute of Applied Physics, Technical University, 1756 Sofia, Bulgaria.

[1] E. Callen and H.B. Callen, Phys. Rev. **139**, A455 (1965).
[2] P.R. Birss, in *Symmetry and Magnetism*, Selected Topics in Solid State Physics, edited by E.P. Wohlfahrt (North-Holland, Amsterdam, 1966), Vol. III, Chap. V, pp. 153–181.
[3] J. Jensen and A.R. Mackintosh, *Rare Earth Magnetism: Structures and Excitations* (Clarendon, Oxford, 1991).
[4] R. Alben and E. Callen, Phys. Rev. **186**, 522 (1969); M.E. Lines, Phys. Rep. **55**, 133 (1979).
[5] K.H.W. Stevens, in *Magnetism*, edited by G. Rado and H. Suhl (Academic, London, 1963), Vol. 1, pp. 1–24.
[6] M.T. Hutchings, in *Solid State Physics*, edited by F. Seitz and D. Turnbull (Academic, New York, 1964), Vol. 16, pp. 227–275.
[7] J. van Vleck, Phys. Rev. **52**, 1178 (1937); J. Phys. Rad. (Paris) **20**, 124 (1959).
[8] F. Keffer, Phys. Rev. **100**, 1692 (1955).
[9] R.A. Tahir-Kheli and H.B. Callen, Phys. Rev. **135**, A679 (1964); H.B. Callen and E.R. Callen, Phys. Rev. **136**, A1675 (1964).
[10] K.-D. Durst and H. Kronmüller, J. Magn. Magn. Mater. **59**, 86 (1986).
[11] R.J. Elliott, in *Magnetic Properties of Rare-Earth Metals*, edited by R.J. Elliott (Plenum, New York, 1972), Chap. 1, pp. 1–16.
[12] W. Wolf, Phys. Rev. **108**, 1152 (1957).
[13] K. Yosida and M. Tachiki, Prog. Theor. Phys. **17**, 331 (1957).
[14] F. Keffer, in *Handbook of Physics*, edited by S. Flügge (Springer, Berlin, 1966), Vol. XVIII/2, pp. 1–273.
[15] H. Callen and S. Shtrikman, Solid State Commun. **3**, 5 (1965).
[16] W. Döring, Ann. Phys. (7)**1**, 102 (1958); in *Handbook of Physics*, edited by S. Flügg (Ref. 14), Vol. XVIII/2, pp.

341–437 and references therein.
[17] J.J. Rhyne and S. Legvold, Phys. Rev. **138**, A507 (1965).
[18] R.J. Elliott and M.F. Thorpe, J. Appl. Phys. **39**, 802 (1968).
[19] Y. Millev and M. Fähnle, J. Magn. Magn. Mater. **135**, 285 (1994).
[20] Y. Millev and M. Fähnle, Phys. Rev. B **51**, 2937 (1995).
[21] Y. Millev and M. Fähnle, Phys. Status Solidi **B 171**, 499 (1992); Am. J. Phys. **60**, 947 (1992).
[22] C. Rudowicz, J. Phys. C **18**, 1415 (1985).
[23] E.R. Callen and H.B. Callen, J. Phys. Chem. Solids **16**, 310 (1960).
[24] Y. Millev and M. Fähnle, Phys. Status Solidi B **182**, K35 (1994).
[25] N. Akulov, Z. Phys. **100**, 197 (1936); C. Zener, Phys. Rev. **96**, 1335 (1954); H.B. Callen and E.R. Callen, J. Phys. Chem. Solids **27**, 1271 (1966).
[26] H.B.G. Casimir, J. Smit, U. Enz, J.F. Fast, H.P.J. Wijn, E.W. Gorter, A.J.W. Duyvesteyn, J.D. Fast, and J.J. de Jong, J. Phys. Rad. (Paris) **20**, 360 (1959).
[27] J.M.D. Coey, Phys. Scr. **T19**, 426 (1987).
[28] J.M. Cadogan, J. P. Gavigan, D. Givord, and H.S. Li, J. Phys. F **18**, 779 (1988).
[29] K.H.J. Buschow, Rep. Prog. Phys. **54**, 1123 (1991).
[30] Y. Millev and M. Fähnle, J. Phys. A **27**, 7235 (1994).
[31] H.B. Callen, Phys. Rev. **130**, 890 (1963); R. Tahir-Kheli, in *Phase Transitions and Critical Phenomena*, edited by C. Domb and M.S. Green (Academic, London, 1975), Vol. 5B, pp. 259–341.
[32] E. du Tremolet de Lacheisserie, *Magnetostriction: Theory and Applications of Magnetoelasticity* (CRC Press, Boca Raton, 1993).
[33] G. Asti, in *Ferromagnetic Materials*, edited by K.H.J. Buschow and E.P. Wohlfahrt (Elsevier, Amsterdam, 1990), Vol. 5, pp. 398–464.
[34] S. Nieber and H. Kronmüller, Phys. Status Solidi **165**, 503 (1991).
[35] R.J. Radwanski and J.J. Franse, J. Magn. Magn. Mater. **74**, 43 (1988); **80**, 14 (1989).
[36] M. Fähnle, K. Hummler, M. Liebs, and T. Beuerle, J. Appl. Phys. A **57**, 67 (1993); in *Computer Aided Innovation of New Materials II, Part 1*, edited by M. Doyama, J. Kihara, M. Tanaka, and R. Yamamoto (Elsevier, Amsterdam, 1993), pp. 209–212.
[37] K. Ried, V. Özpamir, and H. Kronmüller, Phys. Rev. B **50**, 10 027 (1994).
[38] K. Hummler, Ph.D. Thesis, University of Stuttgart, 1994.
[39] D. Givord, H.S. Li, and R. Perrier de la Bathie, Solid State Commun. **51**, 857 (1984).
[40] M. Yamada, H. Kato, H. Yamamoto, and Y. Nakagawa, Phys. Rev. B **38**, 620 (1988).
[41] Magnetoelastic contributions might lead to the emergence of a term $K_4 \sin^8 \theta$, much like in the case of Tb (Ref. 3).
[42] M. Liebs, K. Hummler, and M. Fähnle, Phys. Rev. **46**, 11 201 (1992).
[43] K.R. Lea, M.J.M. Leask, and W.P. Wolf, J. Phys. Chem. Solids **23**, 1381 (1962); J. Shouting, L. Hua, and G. Ruwei, J. Magn. Magn. Mater. **136**, 294 (1994); R.R. Sobral, A.P. Guimarães, and X.A. da Silva, J. Magn. Magn. Mater. **137**, 186 (1994).